Int. J. Electrochem. Sci., 13 **(2018)** 10496 – 10513, doi: 10.20964/2018.11.47

International Journal of ELECTROCHEMICAL SCIENCE
www.electrochemsci.org

Mini review

Electrochemical Biosensors with Electrocatalysts Based on Metallic Nanomaterials as Signal Labels

Lin Liu[1,*], *Dehua Deng*[1,2], *Wenfeng Sun*[1], *Xiaohui Yang*[1], *Suling Yang*[1,*] *and Shijie He*[1]

[1] Henan Province of Key Laboratory of New Optoelectronic Functional Materials, College of Chemistry and Chemical Engineering, Anyang Normal University, Anyang, Henan 455000, People's Republic of China
[2] College of Chemistry and Chemical Engineering, Henan University, Kaifeng, Henan 475001, People's Republic of China
[*]E-mail: liulin@aynu.edu.cn (L.L.); yang_suling@163.com (S.Y.)

Received: 21 June 2018 / *Accepted:* 2 September 2018 / *Published:* 1 October 2018

In recent years, metallic nanomaterials have been widely used in the field of electric sensing due to their superior physical and chemical properties. They can serve as the electrode modifiers to enhance electron transfer, as carriers to load signal markers such as enzyme and redox reporters, or directly as the reporters for signal readout. In particular, metallic nanomaterials as electrocatalysts have become much-favored tools in electrochemical bioassays. In this review, the progress in metallic nanaoelectrocatalysts-based biosensors was addressed.

Keywords: Metallic nanomaterials; electrochemical biosensors; electrocatalysts

1. INTRODUCTION

In recent decades, electrochemical biosensors have been attractive for a broad range of applications in clinical diagnosis, biomedical research, food quality control and environmental monitoring taking the advantage of their exceptional attributes (e.g. simplicity, rapid response, and compatibility with miniaturization) [1, 2]. To improve the detection sensitivity, considerable attention has been devoted to the integration of recognition elements with electronic elements to prepare the detection/signal probes, including enzymes, carbon nanomaterials, metal nanoparicles, metallic oxides and sulfides, and nanocomposites. To date, enzyme-based signal amplification with horseradish peroxidase (HPR), alkaline phosphatase (ALP) or glucose oxidase (GOx) as the label is still one of the most common high-efficiency strategies in electrochemical sensing devices. In particular, the devices

entailing multiple signal amplification such as enzyme-loaded nanomaterials and enzymatic reaction plus redox cycling greatly improve the sensitivity [1]. However, their applications in practice are still limited because of the time consuming detection procedure, the costly and complicated preparation process, the cross-talk interference, and/or the requirement of a deoxygenation process to exclude the interference of dissolved oxygen [3, 4]. Nanomaterials as signal labels without enzyme modification have numerous remarkable merits to improve the sensitivity. In general, nanomaterials can be exploited as nanocarriers to load signal markers or directly used as signal reporters [5-10]. Because metal atoms can be determined by anodic stripping voltammetry and each nanoparticle contains thousands of metal atoms, metallic nanoparticles and their compounds are often employed as nanoprobes to amply the signal. The detection principle and emerging trends have been introduced in recent review papers [11-13]. Besides, metallic nanomaterials can accelerate the electron transfer rate and exhibit fascinating catalytic activities [14, 15]. Recently, metallic nanomaterials have been widely employed as electrocatalysts to enlarge the electrochemical signal and avoid the shortcoming of enzymes such as thermal and environmental instability. Herein, we offered a comprehensive review of metallic nanoelectrocatalysts-based biosensors.

2. METALLIC NANOELECTROCATALYSTS

2.1 Metallic nanoparticles

2.1.1 Gold

As one of the most popular nanomaterials, gold nanoparticles (AuNPs) have been recognized as excellent candidates for developed non-enzymatic electrochemical biosensor due to their larger surface-to-volume ratio and the interface-dominated properties. In the past years, numerous research teams have developed novel and efficient signal-amplified biosensors based on the good electrocatalytic property of AuNPs [16, 17]. An interesting work using gold nanopartilces as the electrocatalysts for signal amplification was first developed by Yang's group (Figure 1) [18]. In this work, AuNPs conjugated with IgG can catalyze the reduction of p-nitrophenol (NP) to p-aminophenol (AP) with the aid of the $NaBH_4$. Moreover, in the presence of $NaBH_4$, the electrochemical catalytic reaction between AP and *p*-quinone imine was initiated with the help of the ferrocene as an electron mediator, producing amplified electrochemical signal. The redox reaction between a highly outer-spherereaction-philic (OSR-philic) species and a highly inner-spherereaction-philic (ISR-philic) species is slow. Furthermore, Yang's group employed OSR- and ISR-philic gold nanocatalysts to mediate both OSR- and ISR-philic species. Under potential conditions, the sandwich-type immunosensor was applied to highly sensitive and incubation-free detection of creatine kinase-MB [19].

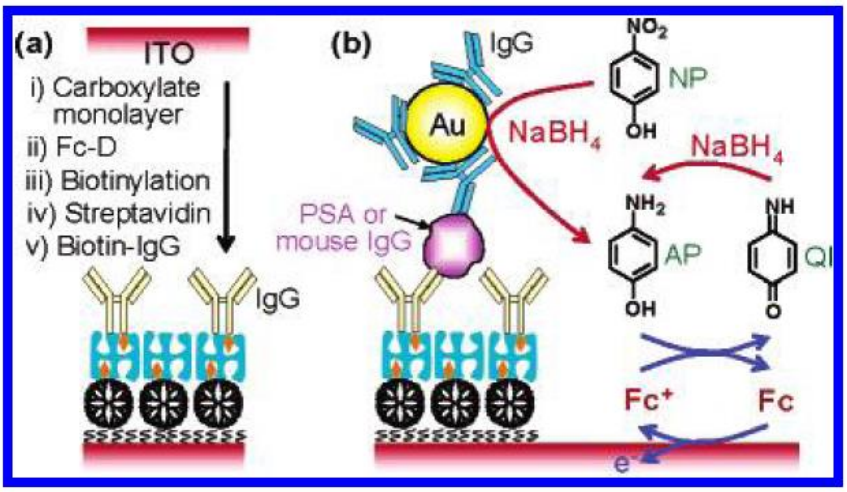

Figure 1. (a) Schematic representation of the preparation of an immunosensing layer. (b) Schematic view of electrochemical detection of mouse IgG or PSA. Reprinted with permission from reference [18]. Copyright 2006 American Chemical Society.

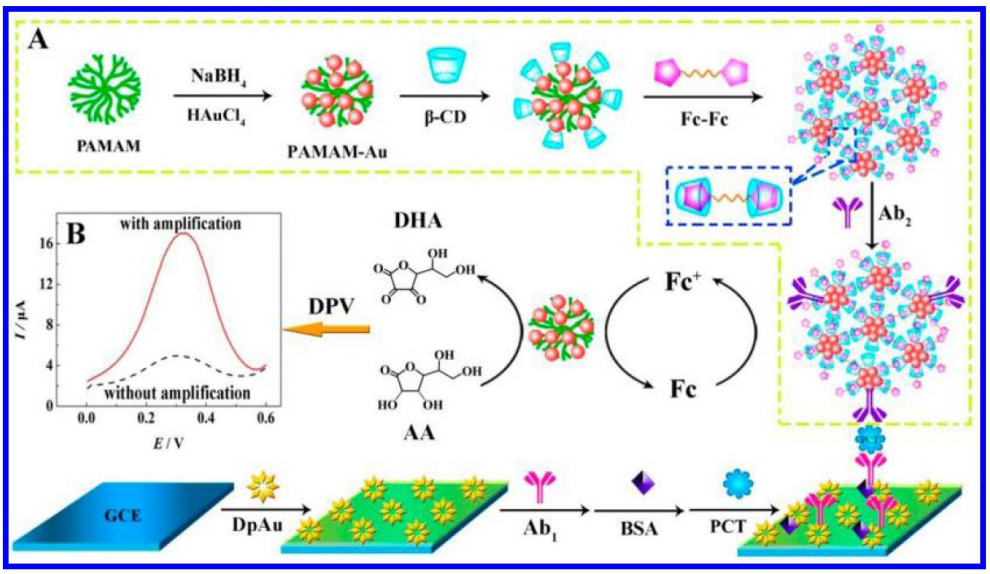

Figure 2. Schematic diagram of fabrication of electrochemical immunosensor. (A) Preparation procedure of Fc-Fc/β-CD/PAMAM-Au-labeled Ab2 bioconjugates. (B) Comparative DPV signals with and without amplification. Reprinted with permission from reference [20]. Copyright 2015 American Chemical Society.

To control the particle size under 10 nm, poly(amidoamine) (PAMAM) dendrimers have been used as the templates to prepare AuNPs that can catalyze the oxidation of NADH and ascorbic acid (AA) or the reduction of H_2O_2. In the case of AA, Yuan's group developed an enzyme-free electrochemical immunosensor for procalcitonin detection using PAMAM-AuNPs as the electrocatalytic labels (Figure 2) [20]. The netlike nanostructure of Fc-Fc/β-CD/PAMAM-AuNPs was formed by N,N-bis(ferrocenoyl)-diaminoethane (Fc-Fc) as an bridge to bring β-CD capped PAMAM-AuNPs together through the host-guest recognition, which is further decorated by secondary antibodies

(Ab_2). In the nanonets, PAMAM-AuNPs were not only used as the nanocarriers to adsorb β-CD and Ab_2, but also as mimic enzymes to catalyze the oxidation of AA. Moreover, Fc-Fc not only acted as an eletroactive group for electrochemical response, but also exhibited catalytic activity towards AA oxidation. The proposed immunosensor shows a wide linear range from 1.80 pg/mL to 500 ng/mL and a low detection limit of 0.36 pg/mL.

2.1.2 Silver

As one of typical nanomaterials, silver-based nanostructure has been applied to modify the electrode surface. The silver nanomaterials exhibit good electrocatalytic activity for H_2O_2, which depend on their dimension and amount deposited on electrode surface. For example, Compton and co-workers reported that AgNPs can be electrochemically deposited on the surface of a gassy carbon electrode for detection of H_2O_2 [21]. The reduction of H_2O_2 is facilitated by modification of the electrode surface with nanosized silver assemblies. This modified nanosilver electrode exhibits a detection limit of 2×10^{-6} mol/L in 50 mM phosphate buffer (pH 7.4). The method shows a higher sensitivity than that achieved at a silver microelectrode. Additionally, highly uniform dendritic silver nanostructure electrodeposited on the glassy carbon electrode was reported by Rezaei and co-workers for the determination of H_2O_2 [22]. Ag nanodendrites was proved to be a superior electrocatalyst and significantly enhance the electron-transfer rate by 1-2 orders of magnitude, mainly due to the presence of the high amounts of sharp edges and defects on the dendrites as electroactive sites along with their large microscopic surface area.

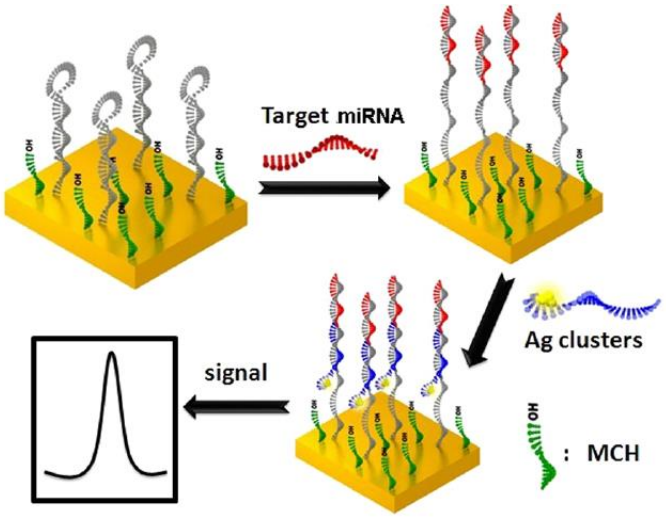

Figure 3..Illustration of electrochemical detection of MiRNA using oligonucleotide encapsulated AgNCs. Reprinted with permission from reference [23]. Copyright 2012 American Chemical Society.

Silver nanoclusters (AgNCs) with larger surface area and more low-coordinated sites have been applied in electrochemical bioassays. Zhang and co-workers first employed silver nanocluster as effective mimic enzymes towards H_2O_2 reduction to construct a sensitive, selective, and label-free electrochemical miRNA biosensor [23]. As shown in Fig.3, the molecular beacon (MB) probes have

two elaborately designed sequences, which can hybridize with the target and functional probes encapsulated AgNCs. After subsequent hybridization of the MB probes with the target and functional probes, the AgNCs were close to the electrode surface and catalyzed the reduction of H_2O_2, producing an amplified electrochemical signal. The superior catalytic property of AgNCs toward H_2O_2 reduction and the selectivity of the MB probes provide the method with a detection limit of 67 fM, which is lower than a native enzyme-based DNA detection system.

2.1.3 Platinum

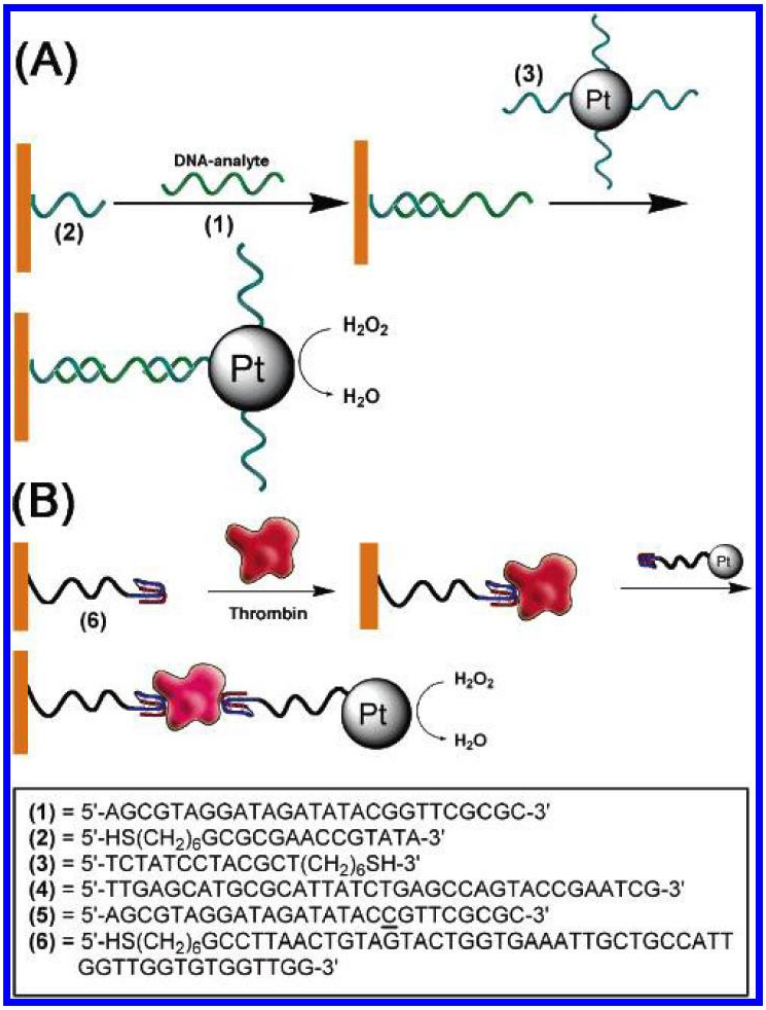

Figure 4. Scheme depicting the analytical procedure for using the PtNPs in the analysis of (A) DNA and (B) thrombin. Reprinted with permission from reference [24]. Copyright 2006 American Chemical Society.

According to the lectures, many amounts of catalytic reactions have been studied including hydrogen, oxygen, H_2O_2 and glucose. Besides Au and Ag, platinum (Pt) nanoparticles (PtNPs) have also been widely exploited to construct electrochemical immunosensors based on its good catalytic properties. Willner's group first demonstrated that PtNPs can act as catalytic labels for the reduction of H_2O_2 to amplify the signal of electrochemical biosensors [24]. When DNA modified PtNPs were tethered to the duplex DNA or the thrombin aptamer/thrombin complex (Figure 4), the

electrocatalyzed reduction of H_2O_2 proceeds near the surface of the electrode, resulting in an electrocatalytic cathodic wave at -0.3V. Finally, the method allowed for amplified detection of DNA and thrombin with the detection limits of 1×10^{-11} M and 1×10^{-9} M, respectively. The values are much lower than those of the previously reported methods. To facilitate the highly sensitive detection of ultralow concentrations of DNA or other biomolecules, Bard et al. demonstrated that PtNPs can be used as the catalysts for hydrazine oxidation at an Au ultramicroelectrode (UME) (Figure 5) [25]. The speed of electrocatalytic oxidation of hydrazine at PtNPs surface is significantly faster than that at bare UME. The single DNA target can induce a collision and adhesion between PtNPs and UME, producing a large current amplification response. Besides Pt nanospheres, other nanostructured Pt materials also exhibit excellent catalytic ability, such as Pt nanocubes and mesoporous nanoparticles. For example, to fabricate the immunosensors, Wei's group employed mesoporous PtNPs (m-PtNPs) as the mimic enzymes for signal amplification detection on a graphene-modified screen printed carbon electrode (SPEC) [26]. After the formation of a sandwich-type complex between antibody and a selected tumor marker, m-PtNPs catalyzed the reduction of H_2O_2 at the electrode surface, producing a strong electrochemical signal.

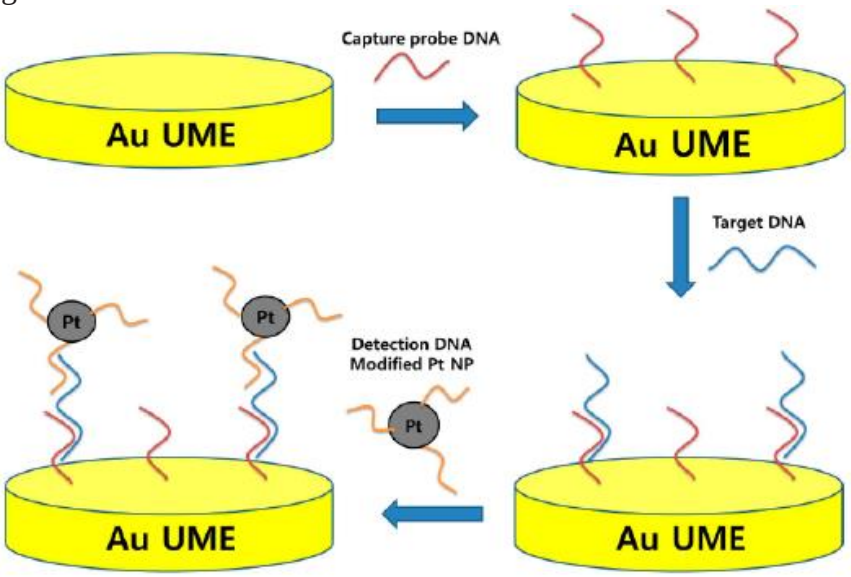

Figure 5. Illustration of sandwich-type DNA sensor on the Au UME (Radius 5 μm). Reprinted with permission from reference [25]. Copyright 2012 American Chemical Society.

2.1.4 Bimetallic and trimetallic nanoparticles

The properties of nanoparticles could be elegant designed by tuning the size, shape, and composition of nanoparticles. Bimetallic and trimetallic nanoparticles have received increasing research interest for biosensing applications because of their prominent catalytic activities and stabilities over monometallic nanoparticles [27-34]. Typically, Ju's group presented a highly sensitive method for chloramphenicol immunoassay based on AuPd bimetallic NPs as the signal tags (Figure 6) [27]. The adamantine (ADA)-labeled antibody (ADA-Ab) competitively bound the antigen immobilized on the electrode and the target in solution. The AuPd bimetallic NPs functionalized with

β-cyclodextrin (β-CD) was bounded to the electrode by a host-guest interaction between β-CD and ADA. AuPd NPs showed efficient electrocatalytic ability for $NaBH_4$ oxidation and produced ultrasensitive response to chloramphenicol. The senor exhibits a wide linear range (50 pg/mL to 50 μg/mL) and a low detection limit (4.6 pg/mL). Lately, the enzyme-free detection of carbohydrate antigen 125 (CA125) by Au@Pd core-shell NPs was reported by the Wei's group [29]. In this study, the monodispersed Au@Pd NPs showed higher electrocatalytic activity toward H_2O_2 reduction by enhancing the electron transfer. Ma's group also fabricated polyaniline decorated-Au/Pd nanocomposites with high eletrocatalytic activity toward H_2O_2 reduction and demonstrated their applications for simultaneous detection of four tumor biomarkers [30].

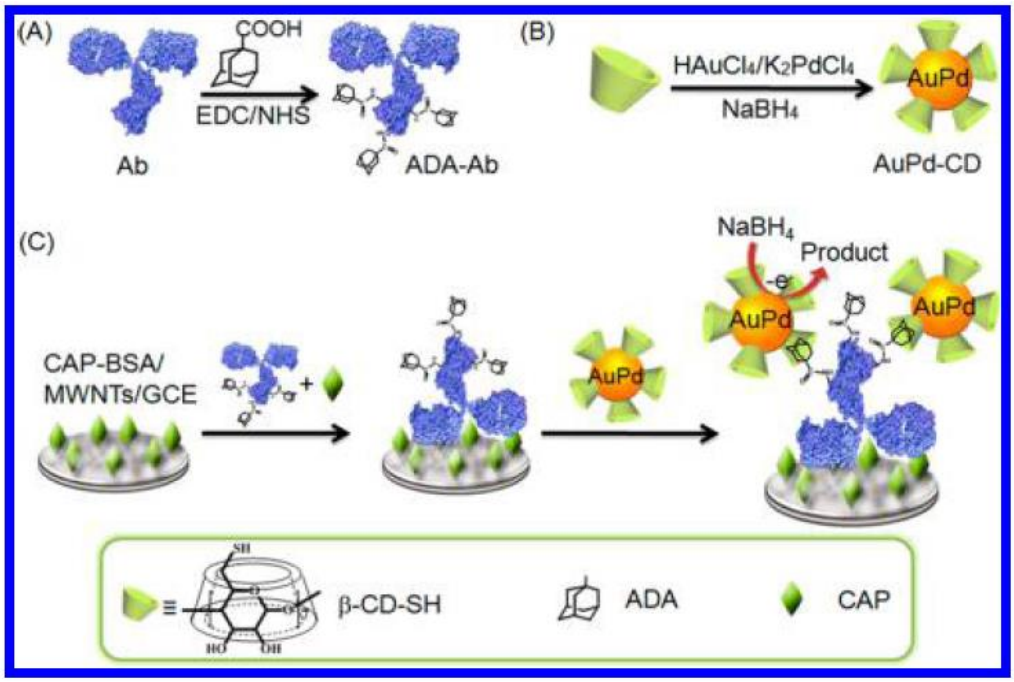

Figure 6. Preparation of (A) ADA-Ab conjugate and (B) β-CD-functionalized AuPd bimetallic nanoparticles, and (C) electrochemical immunoassay procedure for the detection of a small molecule. Reprinted with permission from reference [27]. Copyright 2013 American Chemical Society.

Furthermore, with bimetallic nanoporous PtFe alloys (NP-PtFe) as signal labels, Wei's group developed an immunosensor for the detection of cancer biomarker carbohydrate antigen 15-3 (CA15-3) [31]. The hierarchical NP-PtFe displayed a high electrocatalytic activity for the electro-oxidation of H_2O_2. The sensor allowed for the detection of CA15-3 ranging from 0.002 to 40 U/mL with a low detection limit (3×10^{-4} U/mL). Additionally, nanoporous PtCo alloys were also applied in Wei's group to determine the zeranol [32]. The nanoporous PtCo alloy, prepared by a dealloying method, showed strong electrocatalytic activity toward the electro-reduction of dissolved oxygen. The nanoporous PtCo alloy loaded with many antibody molecules on each immunoconjugate amplified the detectable signal. The immunosensor exhibited a high sensitivity to zeranol with a detection limit of 13 pg/mL. Furthermore, Wei and co-workers demonstrated that trimetallic AuPdPt nanoparticles and ternary Pt-Co-Cu nanodendrites can accelerate the electron transfer and act as the signal labels of

electrochemical immnosensors [33, 34]. These works are valuable for the development of novel electrochemical nanocatalysts.

2.2 Metal composite carbon materials

Carbon materials, such as graphene, carbon nanotubes (CNTs) and mesoporous carbon (MSC), have many advantages, including favorable electron conductivity, large surface area, and ease of manipulation as well as biocompatibility [1]. Therefore, there has been a worldwide interest in the application of carbon materials for biosensors development. In particular, carbon materials hold great potentials as the supports to disperse and stabilize metal, metal oxide and semiconductor nanomaterials, which expand the synergistic electrocatalytic and optoelectronic properties.

2.2.1 Graphene as the support

Graphene is a single-atom-thick 2D material. Because of the high electron transfer rate, versatile surface modification and high surface area, graphene and its derivatives including graphene oxide (GO) and reduced graphene oxide (rGO) have been widely used as the supports to construct biosensors [31, 35-38]. For example, Lin's group prepared an efficient mimic enzyme using GO support for loading of PtNPs, which possessed significantly enhanced peroxidase-like catalysis and electrocatalysis ability [35]. In this elegant nanocomposites, GO were first used for the dispersion of CNTs and then the *in situ* decoration of PtNPs by the impregnation method using H_2 as the reducing agent. The synthesized GO-CNT-Pt nanocomposites were successfully employed to detect H_2O_2 in the presence of 3,3′,5,5′-tertamethylbenzidine (TMB), through a sandwiched electrochemical immunoassay. Wang et al. developed an electrochemical immunosensor for CEA detection with AgNCs/GO as the signal label to promote the electrochemical reduction of H_2O_2. The proposed biosensor shows a linear range of 0.1 pg/mL ~ 100 ng/mL and a detection limit of 0.037 pg/mL [38].

Du and co-workers prepared a sensitive sandwich-type biosensor for AFP detection using PdNi alloy nanoparticles decorated with secondary anti-AFP-conjugated N-doped graphene nanoribbons (PdNi/N-GNRs) as signal amplification labels [31]. The GNRs not only improved the catalytic activity towards the reduction of H_2O_2, but also facilitated the immobilization of large numbers of Ab_2 molecules, resulting in a higher sensitivity of sensor. The adamantine-1-carboxylic acid functionalized primary anti-AFP (ADA-Ab_1) was bounded to the β–cyclodextrins functionalized graphene sheets (CD-GS) by the host–guest interaction. This method has good sensitivity with a detection limit of 0.03 pg/mL.

In addition to metal nanoparticles/GO hybrids, other metallic nanoparticles can also be grown *in situ* on the surface of GO. For example, Ge and Song demonstrated that CuS can be *in situ* grown on the surface of ultrathin gold nanowire functionalized graphene sheets [36]. The oxygen-containing functional groups on GO provide multiple binding sites for Cu^{2+} ions, which controlled the deposition of the CuS nanoparticles from aggregation. The fabricated CuS/GO nanocomposites exhibit enhanced electrocatalytic activity toward the reduction of H_2O_2. Based on the 3D paper-based analytical device,

this sensor presented a wide calibration range (0.001 ~ 10 ng/mL) and a low detection limit of 0.5 pg/mL, which meets the demand of AFP monitoring in clinical diagnostics.

2.2.2 CNT as the support

CNTs including single-wall (SWCNTs) and multi-wall (MWCNTs) species are well-ordered and hollow graphitic nanomaterials made up of cylinders of sp^2-hybridized carbon atoms. To enhance their electrochemical behavior, CNTs can be functionalized with other functional materials, such as metal nanoparticles, organic molecules, and conducting polymers. For example, nickel-based nanomaterials play an important role in synthesizing CNT-based hybrids due to the low-cost and outstanding catalytic behavior of nickel. Tang's group reported an enzyme-free electrochemical approach for the detection of PSA, using NiCoBP-doped MWCNT (NiCoBP-MWCNT) as the signal transducer [39]. In this study, MWCNT was first doped by NiCoBP through an induced electroless-plating technique and subsequently conjugated with anti-PSA antibody. The as-prepared NiCoBP–MWCNT showed outstanding oxidase-like ability to catalyze the glucose oxidation with a well-defined redox peak. The PSA biosensor exhibited a good linear response from 0.1 to 50 ng/mL with a high sensitivity (0.035 ng/mL).

2.2.3 Mesoporous carbon as the support

As one of the most fascinating carbon materials, MSC have initiated significant interest in many applications from drug delivery, energy storage, gas storage hosts and catalyst supports because of their large volume-to-surface ratio, high electric conductivity and chemical stability [40, 41]. The synthesized MSC-based hybrids with metal nanostuctures have improved the electrocatalytic properties. An recent example of a MSC-based electrochemical immunosensor for the detection of brevetoxin B (BTB) was reported by Tang's group [40]. In the assay, MSC-enriched palladium nanostructures (MSC-PdNS) were formed by the *in situ* reduction method and the self-assembly technique, and further functionalized with polyclonal rabbit anti-BTB antibody. The nanocomplexes were found to have high efficiency in the catalytic reduction of H_2O_2 as the signal amplification labels. The assay device was conducted on the BTB-BSA-immobilized electrode based on the competitive-type displacement reaction. Under optimal conditions, this enzyme-free sensor exhibited wide linear response for BTB with a detection limit of 5.0 pg/mL, which was lower than that of the commercialized BTB ELISA kits (0.05 ng/mL). Additionally, Bian's group reported a nonenzymatic PdNPs/MSC system to detect H_2O_2 [42]. The PdNPs growed *in situ* within the ordered mesoporous channels and on the surface of MSC showed high catalytic efficiency in H_2O_2 reduction, resulting in the high sensitivity and wide linear range from 7.5 μM to 10 mM.

2.3 Metal-coated magnetic nanospheres

Magnetic nanoparticles have attracted tremendous interest in biomedical applications, such as drug delivery, magnetic resonance imaging, and biological isolation and separation. Since it was

reported that Fe_3O_4 NPs possess an intrinsic horseradish peroxidase-mimicking activity, various Fe_3O_4 NPs-based nanocomposites have been extensively utilized to catalyze the chemical or electrochemical reduction of H_2O_2. According to the reports, the composites of Fe_3O_4 NPs with metal nanoparticles (NPs), in particular noble metal NPs (e.g. gold, palladium, platinum and bimetal) [43, 44], show enhanced catalytic activity than the single-component NPs. The electrochemical biosensors with metal-coated magnetic nanospheres as signal labels have been introduced as follows.

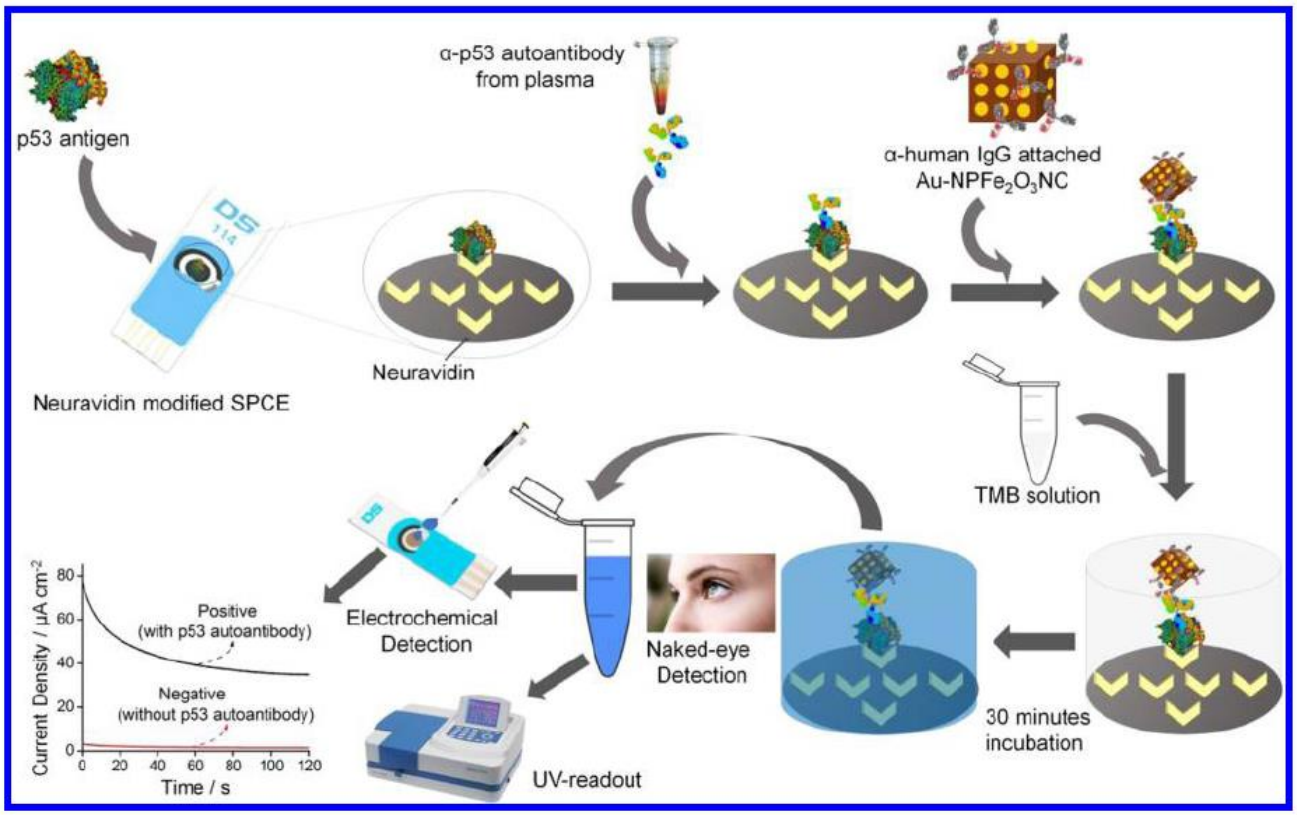

Figure 7. Schematic representation of the assay for the detection of tumor-associated plasma (and serum) p53 autoantibody. A neuravidin-modified screen-printed carbon electrode was functionalized with biotinylated p53. Serum/plasma samples containing p53-specific autoantibody were then incubated onto the electrode surface followed by the incubation with IgG/Au-NPFe_2O_3NC nanocatalysts. The surface-attached Au-NPFe_2O_3NC nanocatalysts catalyzed the oxidation of TMB in the presence of H_2O_2 and produced a blue-colored complex product (naked eye), which turned yellow after the addition of an acid to the reaction media. The level of p53 autoantibody was detected via measuring the intensity (UV-vis) and amperometric current generated by the yellow product. Reprinted with permission from reference [44]. Copyright 2017 American Chemical Society.

Sun et al. synthesized dumbbell-like Au-Fe_3O_4 NPs to investigate the synergetic effect in electrocatalytic reduction of H_2O_2 [45]. The 6 nm Au seeding NPs were first synthesized and then were used as seeds to facilitate the nucleation and growth of Fe on the surface followed by air oxidation. The as-synthesized Au-Fe_3O_4 NPs exhibited stronger electrocatalytic property than single-component Au or Fe_3O_4 NPs due to the polarization effect at the Au-Fe_3O_4 NPs nanoscale interface. Recently, Shiddiky's group demonstrated the use of gold-loaded nanoporous ferric oxide nanocubes (Au-

$NPFe_2O_3NC$) to detect autoantibodies with enhanced electrocatalytic and colorimetric (naked eye) performance (Figure 7) [44]. Au-$NPFe_2O_3NC$ displayed better peroxidase-like activity than natural peroxidase (HRP) toward the catalytic oxidation of 3,3′,5,5′-tertamethylbenzidine (TMB) in the presence of H_2O_2 at room temperature. The enhanced response was mainly due to the high surface of Au-$NPFe_2O_3NC$ and the contribution of the loaded AuNPs. The fabricated nanoprobe had an excellent detection sensitivity (0.08 U/mL) and good reproducibility by the electrochemical readout. Moreover, the proposed method allowed for the determination of p53 autoantibodies in patients' plasma samples with satisfying sensitivity and specificity.

Wei's group developed a sandwich-type immunosensor by employing Pd nanotubes-functionalized magnetic graphene sheet (Pd-Fe_3O_4-GS) as the matrix to immobilize Ab_1 and silicon dioxide (SiO_2) as the labels to conjugate with Ab_2 [46]. Pd-Fe_3O_4-GS possessed high electrochemical catalytic ability towards the reduction of H_2O_2 due to the synergetic effect between Pd nanocubes and Fe_3O_4-GS. After the combination of antibodies and antigens, the steric hindrance of the SiO_2-Ab_2 conjugate would effectively hamper the electron transfer, resulting in the decrease of the amplified electrocatalytic current response. The immunosensor exhibited an ultrasensitive and specific determination of IgG with a detection limit of 3.2 fg/mL. At the same time, Du's group reported an ultrasensitive immunoassay for quantitative determination of AFP [47]. The Pd nanoparticles and Ab_2 was anchored on carbon decorated Fe_3O_4 magnetic microspheres (Fe_3O_4@C). The carbon in Fe_3O_4@C acted as a electron mediator to accelerate the electron transfer. Primary antibodies were immobilized on the carboxyl-functionalized multi-walled carbon nanotubes (MWCNTs-COOH). The high electrocatalytic activity for H_2O_2 reduction and the ease of magnetic separation provide the method with a wide linear range and a low detection limit.

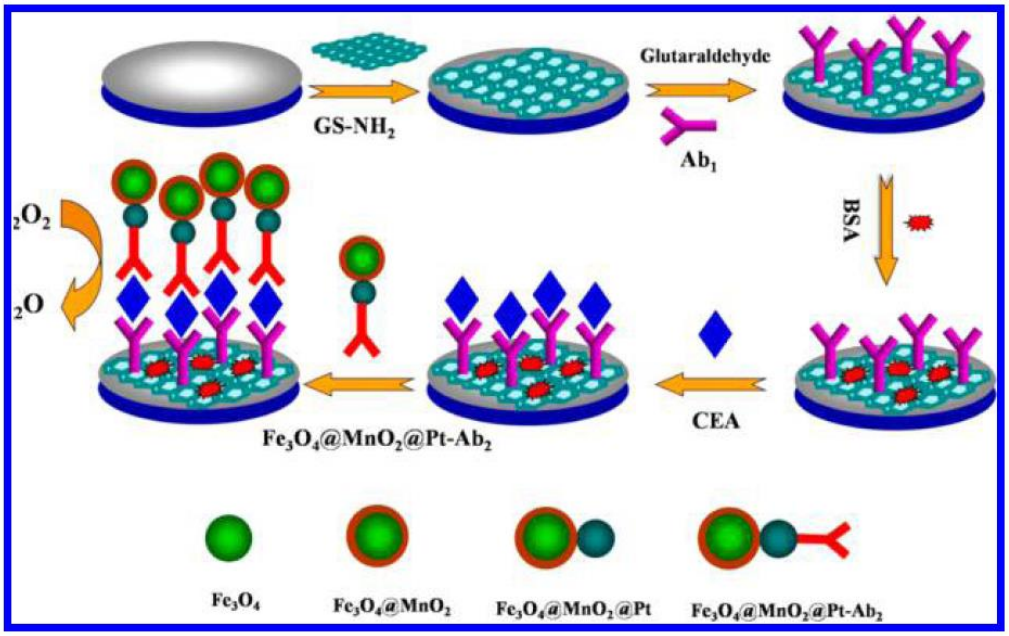

Figure 8. Schematic representation of the preparation process of the immunosensor. Reprinted with permission from reference [48]. Copyright 2014 American Chemical Society.

Yuan and co-workers designed a novel dual signal amplification methodology based on hollow PtNPs-decorated Fe_3O_4 NPs (HPtNPs-Fe_3O_4) and glucose oxidase (GOD) to detect AFP (Figure 8) [48]. Both HPtNPs and Fe_3O_4 have peroxidase-like catalytic ability to amplify the electrochemical signal. The composite of HPtNPs-Fe_3O_4 and GOD can form a pseudo-bienzymatic system. The immunoassay exhibited a linear range of 0.01 ~ 60 ng/mL with a low detection limit of 1.6 pg/mL. Using corallite-like Fe_3O_4@MnO_2@Pt NPs and aminated graphene sheets (GS-NH_2), Wei's group developed an electrochemical immunosensor for the sensitive detection of carcinoembryonic antigen (CEA) [49]. The Fe_3O_4@MnO_2@PtNPs were synthesized and used as labels to conjugate with a secondary antibody. The thin-layer MnO_2 sheets can not only catalyze H_2O_2 reduction, but also possess a large surface area to closely interact with the Fe_3O_4 NPs and PtNPs. The synergetic effect between PtNPs, Fe_3O_4 NPs, and MnO_2 NPs improved the reduction ability of nanolabels toward H_2O_2. Additionally, the GS-NH_2 facilitated the electron transfer because of its excellent electric conductivity. The immunosensor exhibited a broad linear range and a low detection limit, which has potential application for the detection of cancer biomarkers.

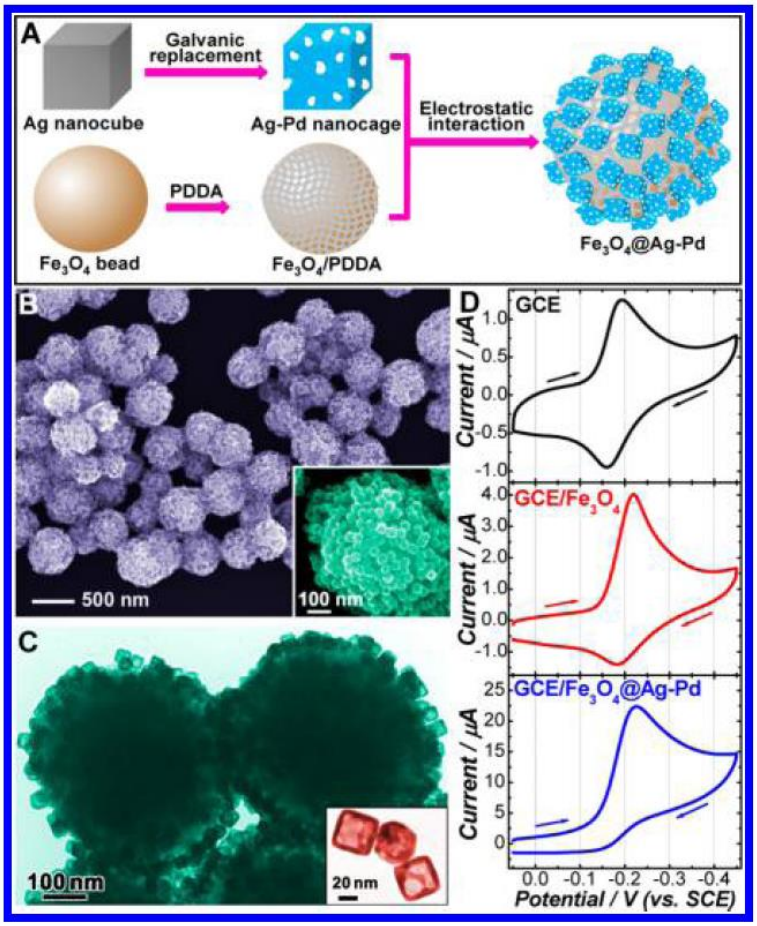

Figure 9. (A) Schematic illustration of the fabrication of Fe_3O_4@Ag-Pd hybrid NPs. (B) SEM image of Fe_3O_4@Ag-Pd hybrid NPs. The inset highlights one Fe_3O_4@Ag-Pd hybrid particle. (C) TEM image of Fe_3O_4@Ag-Pd hybrid NPs. The inset shows a TEM image of Ag-Pd nanocages. (D) CVs of a bare GCE, GCE/Fe_3O_4, and GCE/Fe_3O_4@Ag-Pd in 0.01MPBS buffer (pH 7.0) containing 25 μMthionine. Scan rate = 50 mV s^{-1}. Reprinted with permission from reference [51]. Copyright 2014 American Chemical Society.

Sun and co-workers prepared dumbbell-like PtPd-Fe_3O_4 NPs with tunable composition for electrochemical sensing of H_2O_2 [50]. The monodisperse $Pt_{48}Pd_{52}$ NPs were first synthesized and then were used as seeds to facilitate the nucleation and growth of Fe on the surface followed by air oxidation. The as-synthesized $Pt_{48}Pd_{52}$-Fe_3O_4 NPs can significantly promote electrochemical reduction of H_2O_2 in contrast to either Fe_3O_4 or $Pt_{48}Pd_{52}$ NPs. The detection limit of the $Pt_{48}Pd_{52}$-Fe_3O_4 NPs was 5 nM, much lower than the present catalysts. The ultrasensitive probe was further employed to real-time detection of H_2O_2 released from Raw 264.7 cells under the stimulation of N-formylmethionyl-leucyl-phenylalanine (fMLP). Very interestingly, Zhu and Wang found that magnetic Fe_3O_4 nanoparticles exhibits an electrocatalytic activity towards the reduction of small dye molecules (Figure 9) [51]. The nanoelectrocatalysts can be directly used as signal labels for ultrasensitive electrochemical cytosensing. In this work, Ag-Pd bimetallic nanocages acting as signal amplifiers were attached onto the surface of Fe_3O_4 for enhancement of the electric signal.

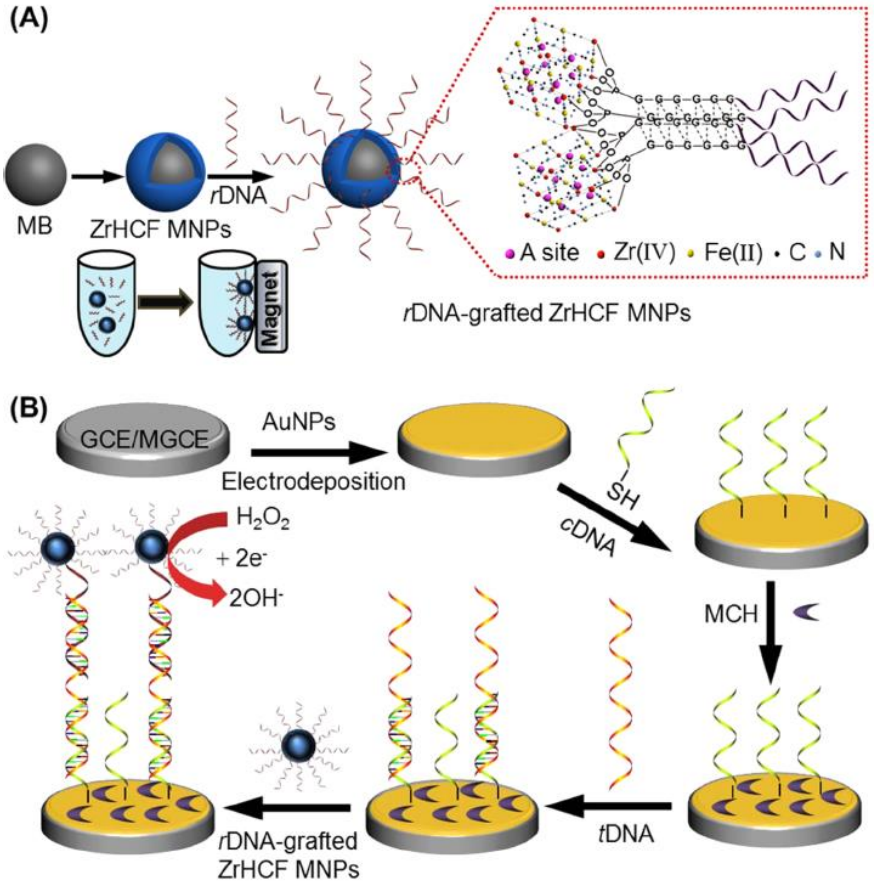

Figure 10. (A) Preparation procedures of rDNA-grafted ZrHCF MNPs. (B) Schematic illustration of the stepwise DNA assay construction process. Reprinted with permission from reference [52]. Copyright 2015 American Chemical Society.

Besides above metal-functionalized MBs, some redox-doped MBs such as thionine and Prussian blue (PB) modified MBs have become quite attractive in electrochemical bioassays. For example, Shan and co-workers designed an electrochemical biosensor for the ultrasensitive DNA assay using multifunctional magnetic zirconium hexacyanoferrate nanoparticles (ZrHCF MNPs) as signal

nanoprobes (Figure 10) [52]. ZrHCF MNPs was made up of magnetic beads (MBs) as inner core and zirconium hexacyanoferrate (II) (ZrHCF) precipitates as outer shell. Zr (IV) could validly adsorb single strand DNA with ployguanines as spacer by the "zirconium-(OPO_3-poly(dG) DNA)" covalent bonds. Moreover, ZrHCF MNPs not only exhibited enhanced electrocatalytic properties towards the reduction of H_2O_2, but also improved the electron transfer ability of the modified electrode. The property of magnetic beads allowed DNA grafted ZrHCF MNPs be obtained by simple magnetic separation. This novel ZrHCF MNPs based strategy presents high sensitivity, excellent selectivity for detecting target DNA and the detection limit was down to 0.43 fM.

2.4 Metal-organic frameworks

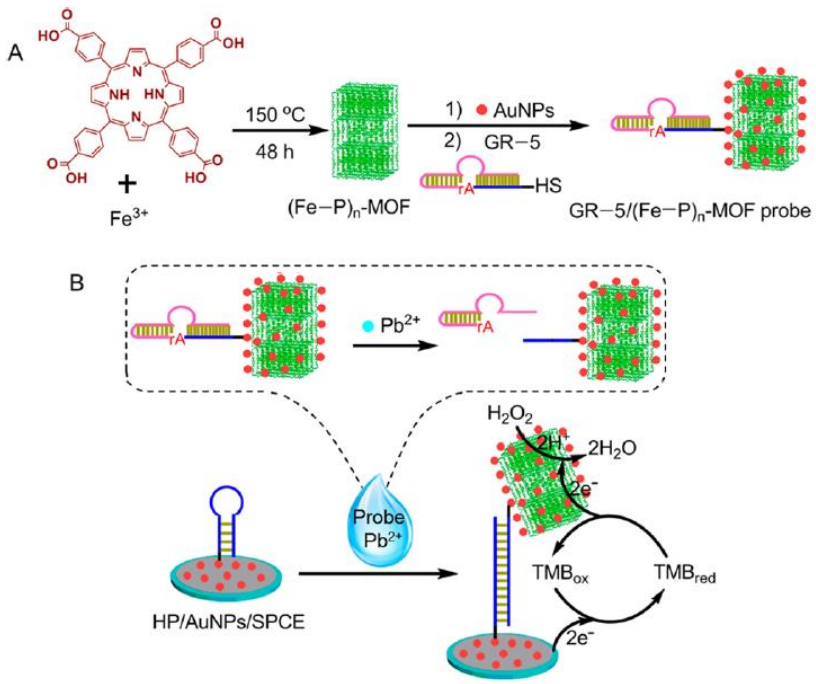

Figure 11. Schematic Representation of (A) Preparation of GR−5/(Fe−P)n-MOF Probe and (B) Electrochemical Detection of Pb^{2+}. Reprinted with permission from reference [54]. Copyright 2015 American Chemical Society.

Metal-organic frameworks (MOFs), formed by metal ions as nodes and organic ligands as linkers by strong covalent bonds, possess favorable physical and chemical properties (e.g. large and permanent inner porosity, high surface areas, and tunable synthesis) [53]. In the past decade, MOFs have attracted widely attention to be applied in catalysis, gas storage, separation, bioimaging, drug delivery, and chemical sensing. Moreover, as cost-efficient and stable enzyme mimic, a series of MOFs have been used as potential materials to design novel biosensors, which have high and specific catalytic activity towards glucose, NADH, O_2 and H_2O_2. Typically, Ju and co-workers have developed several electrochemical biosensors for the detection of DNA, Pb^{2+} and telomerase activity using MOFs as signal labels [54-56]. For example, using a DNAzyme-functionalized iron-porphyrinic metal-

organic framework (GR-5/(Fe-P)$_n$-MOF) as the label, Pb^{2+} was electrochemically detected (Figure 11). In the presence of Pb^{2+}, the GR-5 substrate strand was specifically cleaved into two pieces at the ribonucleotide site. The resulting short (Fe-P)$_n$-MOF-labeled oligonucleotide fragment was released and then hybridized with hairpin probe at the sensor surface. The captured (Fe-P)$_n$-MOF catalyzed the oxidation of TMB in the presence of H_2O_2, resulting in an increase in the reduction peak current.

Using Cu-based metal-organic frameworks (Cu-MOFs) as a mimic glucose-oxidase, Yuan's group has fabricated a highly sensitive ratiometric electrochemical aptasensor for lipopolysaccharide (LPS) detection (Figure 12) [57]. In this work, Cu-MOFs was prepared by $Cu(NO_3)_2$ and 2-amino terephthalic acid through a hydrothermal method and further in situ decorated by AuNPs to immobilize hairpin probes 3 (HP3) on the surface. The resulting Cu-MOFs act as electroactive materials for signal readout. Specifically, the ferrocene (Fc)-labeled hairpin probes 2 (Fc-HP2) was in the "closed" state, inhibiting the interaction with HP3 and making Fc close to the electrode surface. When target LPS was added in the presence of phi29, the cycle I was initiated. This produced a large amount of output DNA which can take part in the N.BstNBI-mediated cyclic II. After few quadratic cycles, a lot of Fc-HP1 was cleaved, resulting in the release of Fc signal molecules from the electrode surface and the exposure of capture probes for hybridization with HP3/AuNPs/Cu-MOFs. The Cu-MOFs in the electrode surface catalyzed the oxidation of glucose, causing the enzyme-free signal amplification. By measuring the peak currents ratio of the Cu-MOFs and Fc, the proposed ratiometric electrochemical assay exhibits improved accuracy and sensitivity.

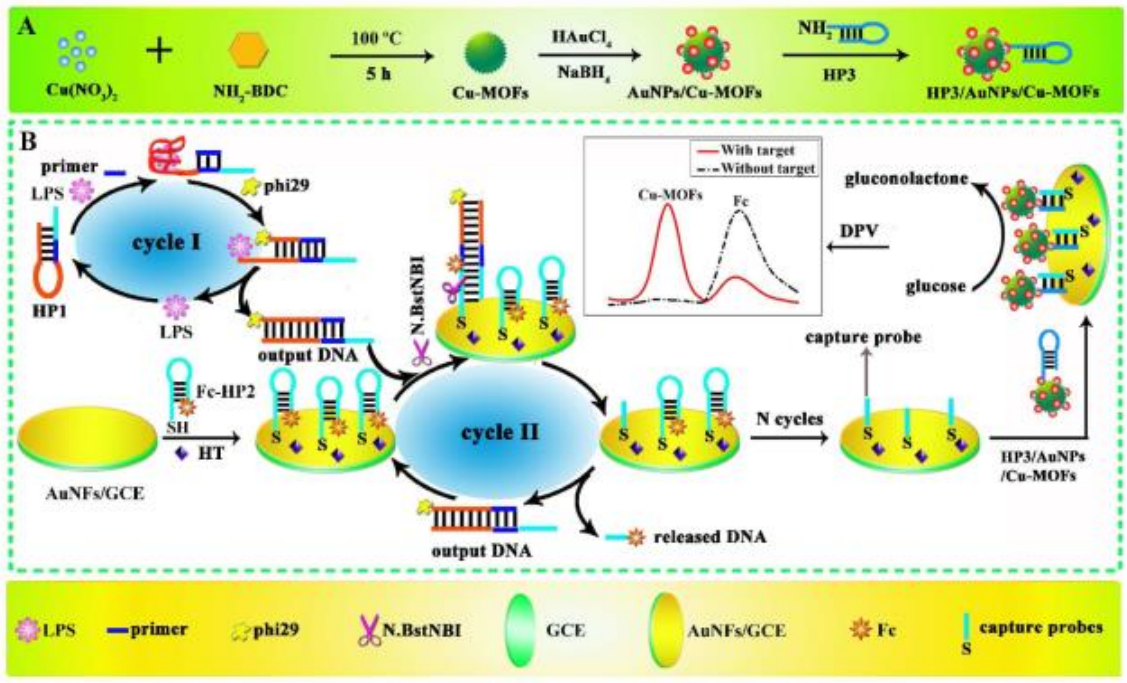

Figure 12. Schematic illustration of the fabrication of the aptasensor: (A) Preparation procedure of HP3/AuNPs/Cu-MOFs; (B) Signal amplification strategy and the detection principle for LPS. Reprinted with permission from reference [57]. Copyright 2015 American Chemical Society.

2.5 Others

The above mimetic catalysts for electrochemical sensing devices provide the advantages of easy production, low cost, high stability and better robustness. However, the reported strategies usually need the use of extra substrates (e.g. glucose and H_2O_2) and/or require redox mediators to facilitate the electron transfer. Water is the reaction medium for most of electrochemical sensors. Our group discovered that the complex formed between Cu(II) and amino terminal Cu(II)- and Ni(II)-binding peptide (ATCUN) exhibits good electrocatalytic ability toward water oxidation [58]. The ATCUN-Cu(II) complex can be attached onto the surface of AuNPs through the Au-S interaction (Figure 13). The resulting nanocatalysts promote the oxidation of water at neural pH with an oxidation potential below 0.85 V, which is lower than that of other Cu(II) complexes-based water oxidation electrocatalysts [59]. With DNA as a model analyte, the sensing device with ATCUN-Cu(II) nanocatalysts showed a detection limit down to 0.1 pM. This is the first electrochemical sensing device with a water oxidation electrocatalyst as the signal label.

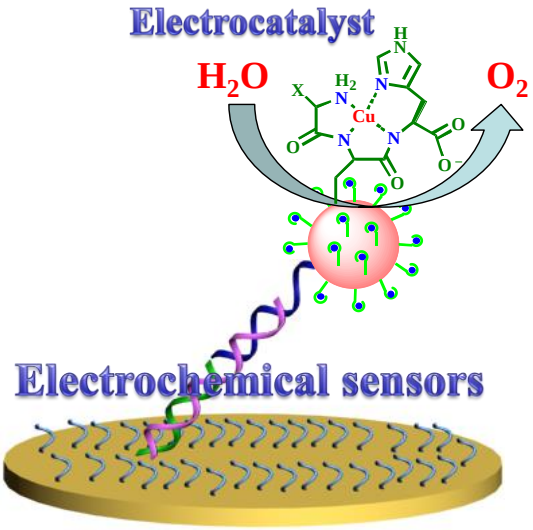

Figure 13. Illustration of sandwich-type DNA sensor with the electrocatalysts as signal labels for water oxidation.

3. CONCLUSION

Metallic nanomaterials can be used as catalysts for electrochemical reaction and organic synthesis. For electrocatalysis-based bioassays, facile electron transfer is dependent upon the distance between electrode and catalysts. Thus, long distance will limit the usefulness of metallic electrocatalysts-based bioassays of proteins and nucleic acids. Another drawback with metallic nanomaterials as labels is that modification of biomolecules on the metal surface may depress their electrocatalytic activity and inhibit the electron transfer. Fortunately, manomaterials can accelerate electron transfer serving as the modifiers of the electrode surface or as electron wires to establish electron communication between electrode and electrochemical labels.

ACKOWLEDGMENTS
Partial support of this work by the National Natural Science Foundation of China (21804002), the fund project for Young Scholar sponsored by Henan province (2016GGJS-122) and the Program for Innovative Research Team of Science and Technology in the University of Henan Province (18IRTSTHN004) is gratefully acknowledged.

References

1. W. Wen, X. Yan, C. Zhu, D. Du and Y. Lin, *Anal. Chem.*, 89 (2017) 138.
2. F. Zhao, C. Cheng and N. Xia, *Int. J. Electrochem. Sci.*, 12 (2018) 7580.
3. Z. Farka, T. Jurík, D. Kovář, L. Trnková and P. Skládal, *Chem. Rev.*, 117 (2017) 9973.
4. B. Yang, J. Li, H. Deng and L. Zhang, *Crit. Rev. Anal. Chem.*, 46 (2016) 469.
5. C. Zhu, G. Yang, H. Li, D. Du and Y. Lin, *Anal. Chem.*, 87 (2015) 230.
6. N. Xia, Z. Chen, Y. Liu, H. Ren and L. Liu, *Sensor. Actuat. B: Chem.*, 243 (2017) 784.
7. N. Xia, X. Wang, B. Zhou, Y. Wu, W. Mao and L. Liu, *ACS Appl. Mater. Interfaces*, 8 (2016) 19303.
8. N. Xia, L. Liu, Y. Chang, Y. Hao and X. Wang, *Electrochem. Commun.*, 74 (2017) 28.
9. J. Wang, G. D. Liu, H. Wu and Y. H. Lin, *Small*, 4 (2008) 82.
10. Y. Chang, M. Wang, L. Wang and N. Xia, *Int. J. Electrochem. Sci.*, 13 (2018) 4071.
11. C. Kokkinos and A. Economou, *Anal. Chim. Acta.*, 961 (2017) 12.
12. C. Kokkinos, A. Economou and M. I. Prodromidis, *TrAC-Trend. Anal. Chem.*, 79 (2016) 88.
13. E. Valera, A. Hernández-Albors and M.-P. Marco, *TrAC-Trend. Anal. Chem.*, 79 (2016) 9.
14. S. Wang, L.-P. Xu and X. Zhang, *Sci. Adv. Mater.*, 7 (2015) 2084.
15. J. Tang and D. Tang, *Microchim Acta*, 182 (2015) 2077.
16. K. Saha, S. S. Agasti, C. Kim, X. Li and V. M. Rotello, *Chem. Rev.*, 112 (2012) 2739.
17. P. A. Rasheed and N. Sandhyarani, *Microchim. Acta*, 184 (2017) 981.
18. J. Das, M. A. Aziz and H. Yang, *J. Am. Chem. Soc.*, 128 (2006) 16022.
19. C. S. Fang, K. H. Oh, A. Oh, K. Lee, S. Park, S. Kim, J. K. Park and H. Yang, *Chem. Commun.*, 52 (2016) 5884.
20. W.-J. Shen, Y. Zhuo, Y.-Q. Chai, Z.-H. Yang, J. Han and R. Yuan, *ACS Appl. Mater. Interfaces*, 7 (2015) 4127.
21. C. M. Welch, C. E. Banks, A. O. Simm and R. G. Compton, *Anal. Bioanal. Chem.*, 382 (2005) 12.
22. B. Rezaei and S. Damiri, *Talanta*, 83 (2010) 197.
23. H. Dong, S. Jin, H. Ju, K. Hao, L.-P. Xu, H. Lu and X. Zhang, *Anal. Chem.*, 84, (2012) 8670.
24. R. Polsky, R. Gill, L. Kaganovsky and I. Willner, *Anal. Chem.*, 78 (2006) 2268.
25. S. J. Kwon and A. J. Bard, *J. Am. Chem. Soc.*, 134 (2012) 10777.
26. Z. Cui, D. Wu, Y. Zhang, H. Ma, H. Li, B. Dua, Q. Wei and H. Ju, *Anal. Chim. Acta*, 807 (2014) 44.
27. L. Wang, J. Lei, R. Ma and H. Ju, *Anal. Chem*, 85 (2013) 6505.
28. X. Zhang, F. Li, Q. Wei, B. Du, D. Wu and H. Li, *Sensor. Actuat. B: Chem.*, 194 (2014) 64.
29. A. Guo, D. Wu, H. Ma, Y. Zhang, H. Li, B. Du and Q. Wei, *J. Mater. Chem. B*, 1 (2013) 4035.
30. L. Wang, F. Feng and Z. Ma, *Sci Rep.*, 5 (2015) 16855.
31. N. Li, H. Ma, W. Cao, D. Wu, T. Yan, B. Du and Q. Wei, *Biosens. Bioelectron.*, 74 (2015) 786.
32. R. Feng, Y. Zhang, H. G. Yu, D. Wu, H. Ma, M., B. C. Zhu, C. X. Xu, H. Li, B. Du and Q. Wei, *Biosens. Bioelectron.*, 42 (2013) 367.
33. F. Shao, L. Jiao, Q. Wei and H. Li, *Microchim. Acta*, 184 (2017) 2031.
34. H. Ma, X. Zhang, X. Li, R. Li, B. Du and Q. Wei, *Talanta*, 143 (2015) 77.
35. H. Wang, S. Li, Y. Si, N. Zhang, Z. Sun, H. Wu and Y. Lin, *Nanoscale*, 6 (2014) 8107.
36. L. Li, L. Zhang, J. Yu, S. Ge and X. Song, *Biosens. Bioelectron.*, 71 (2015) 108.

37. L. Tian, L. Liu, Y. Li, Q. Wei and W. Cao, *Sci. Rep.* (2016)
38. J. Wang, X. Wang, S. Wu, J. Song, Y. Zhao, Y. Ge and C. Meng, *Anal. Chim. Acta*, 906 (2016) 80.
39. B. Zhang, Y. He, B. Liu and D. Tang, *Anal. Chim. Acta*, 851 (2014) 49.
40. Y. Lin, Q. Zhou, Y. Lin, M. Lu and D. Tang, *Anal. Chim. Acta*, 887 (2015) 67.
41. L. Liu, Y. Chao, W. Cao, Y. Wang, C. Luo, X. Pang, D. Fan and Q. Wei, *Anal. Chim. Acta*, 847 (2014) 29.
42. X. Bian, K. Guo, L. Liao, J. Xiao, J. Kong, K. Ji and B. Liu, *Talanta*, 99 (2012) 256.
43. M. K. Masud, M. N. Islam, M. H. Haque, S. Tanaka, V. Gopalan, G. Alici, N.-T. Nguyen, A. K. Lam, M. S. A. Hossain, Y. Yamauchi and M. J. A. Shiddiky, *Chem. Commun.*, 53 (2017) 8231.
44. M. K. Masud, S. Yadav, M. N. Islam, N. T. Nguyen, C. Salomon, R. Kline, H. R. Alamri, Z. A. Alothman, Y. Yamauchi, M. S. A. Hossain and M. J. A. Shiddiky, *Anal. Chem.*, 89 (2017) 11005.
45. C. Xu, J. Xie, D. Ho, C. Wang, N. Kohler, E. G. Walsh, J. R. Morgan, Y. E. Chin and S. Sun, *Angew. Chem. Int. Ed.*, 47 (2008) 173.
46. Y. Wang, H. Ma, X. Wang, X. Pang, D. Wu, B. Du and Q. Wei, *Biosens. Bioelectron.*, 74 (2015) 59.
47. L. Ji, Z. Guo, T. Yan, H. Ma, B. Du, Y. Li and Q. Wei, *Biosens. Bioelectron.*, 68 (2015) 757.
48. Z. Yang, Y. Chai, R. Yuan, Y. Zhuo, Y. Li, J. Han and N. Liao, *Sensor. Actuat. B: Chem.*, 193 (2014) 461.
49. D. Wu, H. Ma, Y. Zhang, H. Jia, T. Yan and Q. Wei, *ACS Appl. Mater. Interfaces*, 7 (2015) 18786.
50. X. L. Sun, S. J. Guo, Y. Liu and S. H. Sun, *Nano Lett.*, 12 (2012) 4859.
51. T. T. Zheng, Q. F. Zhang, S. Feng, J. J. Zhu, Q. Wang and H. Wang, *J. Am. Chem. Soc.*, 136 (2014) 2288.
52. G.-Y. Zhang, S.-Y. Deng, W.-R. Cai, S. Cosnier, X.-J. Zhang and D. Shan, *Anal. Chem.*, 87 (2015) 9093.
53. T. Z. Liu, R. Hu, X. Zhang, K. L. Zhang, Y. Liu, X. B. Zhang, R. Y. Bai, D. Li and Y. H. Yang, *Anal. Chem.*, 88 (2016) 12516.
54. L. Cui, J. Wu, J. Li and H. Ju, *Anal. Chem.*, 87 (2015) 10635.
55. P. Ling, J. Lei, L. Zhang and H. Ju, *Anal. Chem.*, 87 (2015) 3957.
56. P. Ling, J. Lei and H. Ju, *Anal. Chem.*, 88 (2016) 10680.
57. W.-J. Shen, Y. Zhuo, Y.-Q. Chai and R. Yuan, *Anal. Chem.*, 87 (2015) 11345.
58. D. Deng, L. Liu, Y. Bu, X. Liu, X. Wang and B. Zhang, *Sensor. Actuat. B: Chem.*, 269 (2018) 189.
59. F. Zhao, T. Sun and N. Xia, *Int. J. Electrochem. Sci.*, 13 (2018) 4601.